Asia-Pacific J. Atmos. Sci., 46(1), 41-51, 2010
DOI:10.1007/s13143-010-0005-1

Characteristics of Rainfall Systems Accompanied with Changma Front at Chujado in Korea

C.-H. You[1], D.-I. Lee[2], S.-M. Jang[2], M. Jang[2], H. Uyeda[3], T. Shinoda[3] and F. Kobayashi[4]

[1]*Atmospheric Environmental Research Institute, Pukyong National University, Busan, Korea*
[2]*Department of Environmental Atmospheric Sciences, Pukyong National University, Busan, Korea*
[3]H*ydrospheric Atmospheric Research Center, Nagoya University, Nagoya, Japan*
[4]*Department of Geoscience, National Defense Academy, Yokosuka, Japan*

(Manuscript received 31 August 2009; revised 16 October 2009; accepted 12 December 2009)

Abstract: The rainy season from June to July in the East Asia is called the Changma in Korea, the Meiyu in China, or the Baiu in Japan. The mesoscale convective systems which occur near a front frequently lead to severe weather phenomenon such as localized gust and heavy rainfall. An intensive field experiment was conducted at Chujado (33.95°N, 126.28°E) to find out the characteristics of the precipitating system using information such as the raindrop size distribution, kinematic features during a Changma period between June 21 2007 and July 11 2007. Different characteristics of three identified rainfall cases in a Changma frontal precipitation system occurred from 5 to 6 July in 2007 at Chujado area have been identified. Based on the radar reflectivity and raingage at Chujado, each rainfall system maintained for 7 hours, 4 hours, and 9 hours, respectively. According to the analysis of a total vertical wind shear (TVWS) and a directional vertical wind shear (DVWS), the temperature gradient was the strongest near the surface and both warm and cold advections were occurred in all cases but at different levels. The deep warm advection was related to the longer rainfall lifetime and stronger rainrate, but smaller raindrop size. The unstable atmospheric condition, which has cold advection at the surface and warm advection in higher level, caused the larger size diameter of raindrop. The echo top height of 30 dBZ was around 6 km in the two rainfall systems and around 4 km in the other one. The number concentrations of raindrop has turning point at the drop size of 2 mm in diameter. The stronger (weaker) updraft and downdraft were also related to the decreased number concentration of smaller (larger) size drops and increased that of the larger (smaller) drops.

Key words: Changma front, Chujado, advection, echo top, drop size distribution, updraft

1. Introduction

The rainy season from June to July over the East Asia is referred to the Changma in Korea, the Meiyu in China, and the Baiu in Japan. During this period the rainfall area elongated from west to east is called the Meiyu-Baiu front or the Changma front. The mesoscale convective system occurred near the front frequently lead to severe weather such as localized gust and heavy rainfall. There have been studies on the frontal heavy precipitation events which sometimes accompany strong wind gusts near those areas (Matsumoto *et al.*, 1970, 1971; Akiyama, 1973). The formation of frontal systems is influenced by the moisture transport and convergence of the air mass around the South China Sea (Ninomiya, 1978; Ninomiya and Akiyama, 1992; Lee *et al.*, 1998; Ding and Chan, 2005).

Several field experiments have been carried out in the East Asia by various organizations of the country at various locations over the region to clarify the structure and evolution of these frontal precipitation systems. In Japan, observation studies of Doppler radars were carried out in Okinawa (1987), Kyushu Island (1988), and Kyushu Island and over the East China Sea (1998-2002) (Ishihara *et al.*, 1992, 1995; Takahashi *et al.*, 1996; Yoshizaki *et al.*, 2000). In China, the South China Sea Monsoon Experiment (SCSMEX) was carried out between 1996 and 2001 (Lau *et al.*, 2000; Ding *et al.*, 2004). The purpose of these experiments is to understand the mesoscale feature of frontal systems formed in the East Asia (Moteki *et al.*, 2004). In Taiwan, TAMEX (Taiwan Area Mesoscale Experiments) was carried out around Taiwan in 1987 (Lin *et al.*, 1991; Ray *et al.*, 1991; Teng *et al.*, 2000). In Korea, the KORMEX (Korean Mesoscale Experiment) was carried out in the middle of Korean peninsula in 1997 and 1998 (Oh *et al.*, 1997) and the KEOP (Korean Enhanced Observing Program) was carried out in the southern part of Korean peninsula from 2001 to present (Choi and Nam, 2006).

These observational studies are very important especially in Korean peninsula because more than half of annual precipitation over the Korean peninsula is occurred during the summer, and a Changma front accompanies a belt-like peak rainfall zone which are developed in the convergence zone between the tropical maritime and continental air mass (Oh *et al.*, 1997). Some heavy rainfall in Korea is developed by mesoscale disturbances in China and then propagates eastward along the frontal system. There have been also many studies on the synoptic conditions

Corresponding Author: Dong-In Lee, Pukyong National University, 599-1, Daeyeon 3-dong, Nam-gu, Busan 608-737, Korea.
E-mail: leedi@pknu.ac.kr

of this heavy rainfall (Kim *et al.*, 1983; Lee *et al.*, 1998).

However, the observational studies are focused on the mesoscale features of Changma front and its background field at the southern part of the Korean peninsula has been rarely studied. There are few studies on finding out the features of the drop size distributions (DSD) respect to the rainfall systems of Changma front. Therefore, in order to find out the mesoscale characteristics of the precipitations and the associated drop size distributions of Changma front, the Global Research Laboratory (GRL) of Korean Ministry of Education, Science & Technology had set up an intensive observation period (here after IOP) at Chujado (33.95°N, 126.28°E) between June 21, 2007 and July 11, 2007. We identified three separate rainfall systems as the Changma front passes over Chujado within 22 hours and analyzed each system.

Section 2 briefly describes the field experiment setup and the methods used for the case analysis. They include the dual Doppler analysis method for kinematic features, directional (total) vertical wind shear for advection (temperature gradient), and the drop size distributions. The synoptic condition and the characteristics of each system are examined in section 3 and summaries and conclusions are presented in section 4.

2. Experiment setup and methods

Several meteorological instruments were installed at Chujado during field observations. The rain gages collected rainfall every 1 minute and radio-sonde was launched every 6 hours. The Precipitation Occurrence Sensor Systems (POSS) was installed to find out microphysical features of the rainfall system. The surface weather chart, S-band Doppler radars and enhanced IR satellite images from MTSAT were deployed. Global reanalysis data from NCEP/NCAR were obtained for the synoptic weather conditions of the system. This reanalysis data are composed of 2.5° × 2.5° grids with 17 vertical levels from 1000 hPa to 10 hPa, every 6 hours. Observation network covers the southwestern coast of the Korean peninsula and the northern part of the East China Sea with 3 Doppler radars, upper-air soundings (Fig. 1).

To observe the kinematic characteristics of the Changma front, dual Doppler radar analysis was carried out using radars at Gosan (33.17°N 126.09°E) and Seongsan (33.23°N 126.52°E). Those data were interpolated to Cartesian grids using the Sorted Position Radar Interpolation (SPRINT) software (NCAR, 1999) and the Custom Editing and Display of Reduced Information in Cartesian Space (CEDRIC) software package (Miller and Fredrick, 1998). The horizontal and vertical grid resolution was 1.0 and 0.5 km, respectively. Particle fall speeds were estimated from the reflectivity (Biggerstaff and Houze, 1991) and vertical velocity was computed from an elastic equations of continuity (O'Brien, 1970). Three components of wind were estimated by dual Doppler analysis using equations presented by Armijo (1969), and Ray *et al.* (1978, 1980).

In order to understand the strength of temperature gradient and warm (or cold) advection the total vertical wind shear (here after, TVWS) and directional vertical wind shear (here after, DVWS) were calculated using radio-sonde data (Neiman, P. J., 2003, personal communication). The temperature gradient and the advection are approximated from geostrophic thermal wind equation on the isobaric layer (Holton, 1979). If the geostrophic vertical wind shear is assumed to be realistic, the temperature gradient and the advection can be calculated from the equation (1) and (2). It means that the TVWS is proportional to the strength of the temperature gradient and the positive (negative) DVWS is related to the warm (cold) advection.

$$\left|\frac{dV}{dz}\right| \equiv \sqrt{\left(\frac{du}{dz}\right)^2 + \left(\frac{dv}{dz}\right)^2} \tag{1}$$

$$\frac{dD}{dz} \equiv -\left(\bar{u}\frac{dv}{dz} - \bar{v}\frac{du}{dz}\right) \tag{2}$$

where, $V = u\hat{i} + v\hat{j}$, $\bar{u} = [u(k+1) + u(k-1)]/2$, $\bar{v} = [v(k+1) + v(k-1)]/2$ k is the vertical layer, and dz is 500 m in this study.

The rain drop size distribution is calculated using the gamma distribution using 3rd, 4th, 6th moments as in equation (3) (Ulbrich, 1983; Kozu and Nakamura, 1991):

$$N(D) = N_0 D^m \exp(-\Lambda D) \tag{3}$$

where, N_0, D, m, and Λ represent intercept, diameter of rain drop, shape, and slope, respectively. The DSDs were obtained from POSS which has 34 channels between 0.34 mm and 5.34 mm.

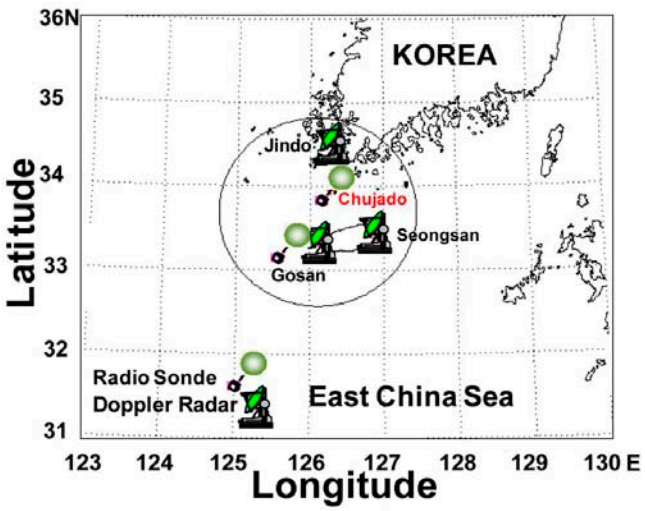

Fig. 1. The location of Doppler weather radar and radio-sonde launch. The circle with 125 km in radius shows the Doppler radar analysis area.

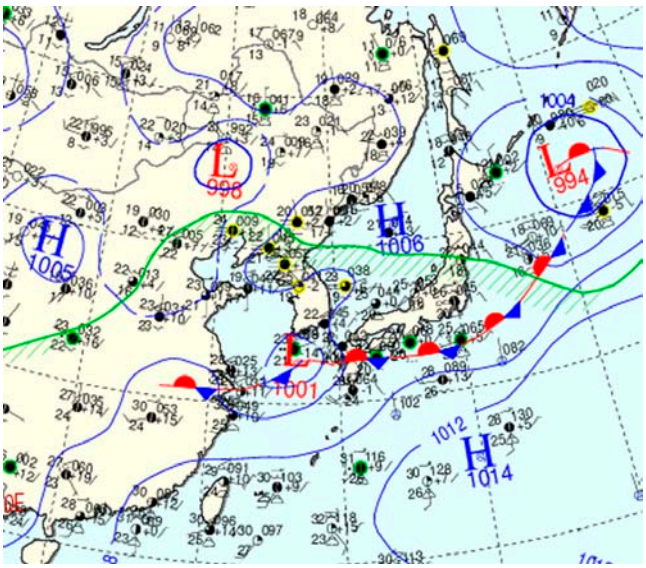

Fig. 2. The surface weather chart on 0900 LST July 6, 2007.

Daily rainfall amount was distributed from 8.6 mm to 92.2 mm. Among these dates, rainfall systems on 5th and 6th July were selected because of its significant rainfall. The rainfall at Chujado was caused by Changma and the presence of strong low pressure (Fig. 2). The vertical profile of reflectivity at Chujado area with time was calculated from Gosan S-band weather radar (Fig. 3). Three different rainfall systems were categorized as follows i.e., 1) the case 1 occurs from 1800 LST 5 July to 0100 LST 6 July ; 2) the case 2 occurs from 0100 to 0500 LST 6 July, and 3) the case 3 occurs 0500 ~ 1400 LST 6 July. The animated weather radar images were used to classify the rainfall system. The system in case 1, case 2, and case3 moved from north-west to south-east, west to east and north-west to north-east, respectively (not shown here).

3. Results

Enhanced IR images from MTSAT-IR shows that the convective

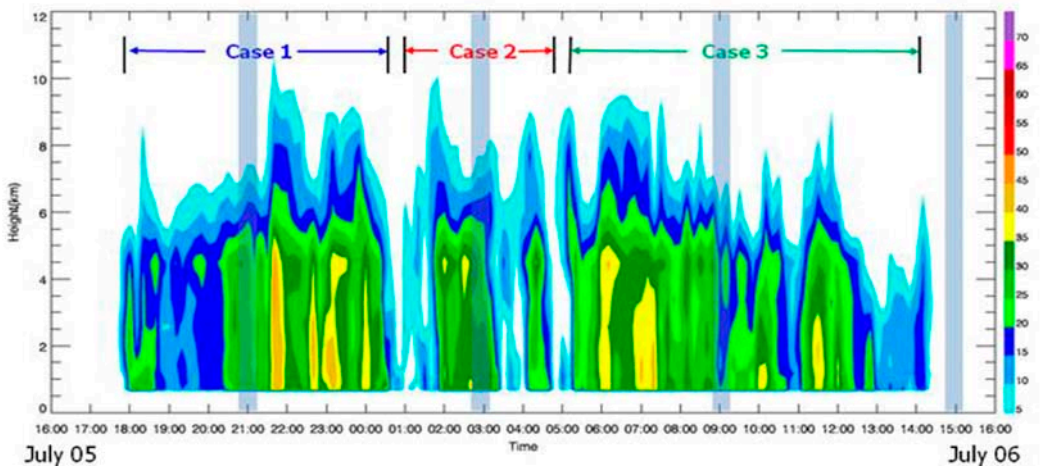

Fig. 3. The vertical profile of reflectivity with time at Chujado obtained from Gosan weather radar. Blue shaded boxes show the timing of radio-sonde launch.

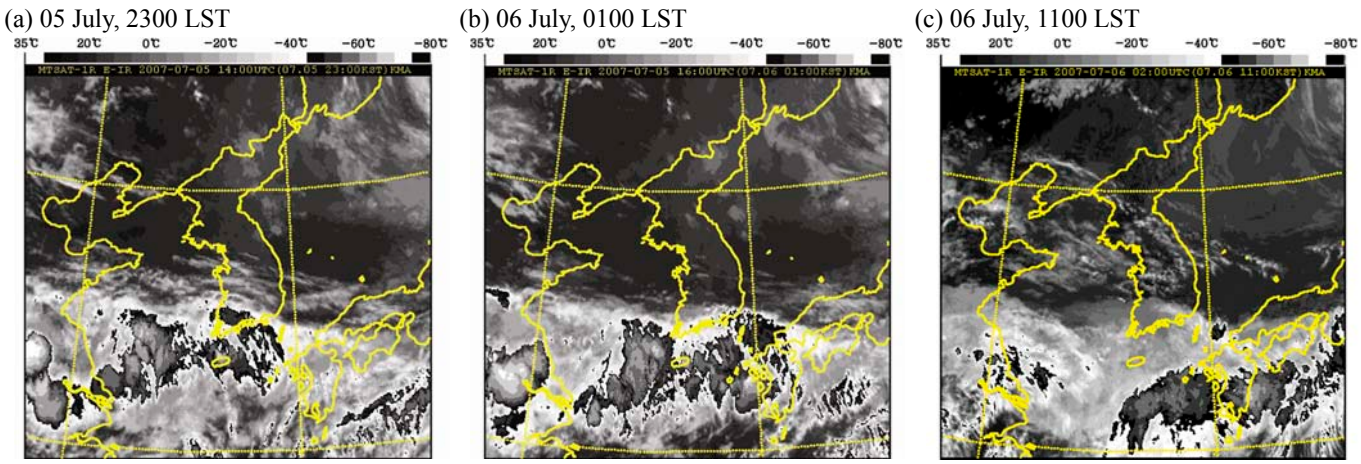

Fig. 4. Enhanced IR images of MTSAT-IR from 2300 LST 5 July to 1100LST 6 July 2007.

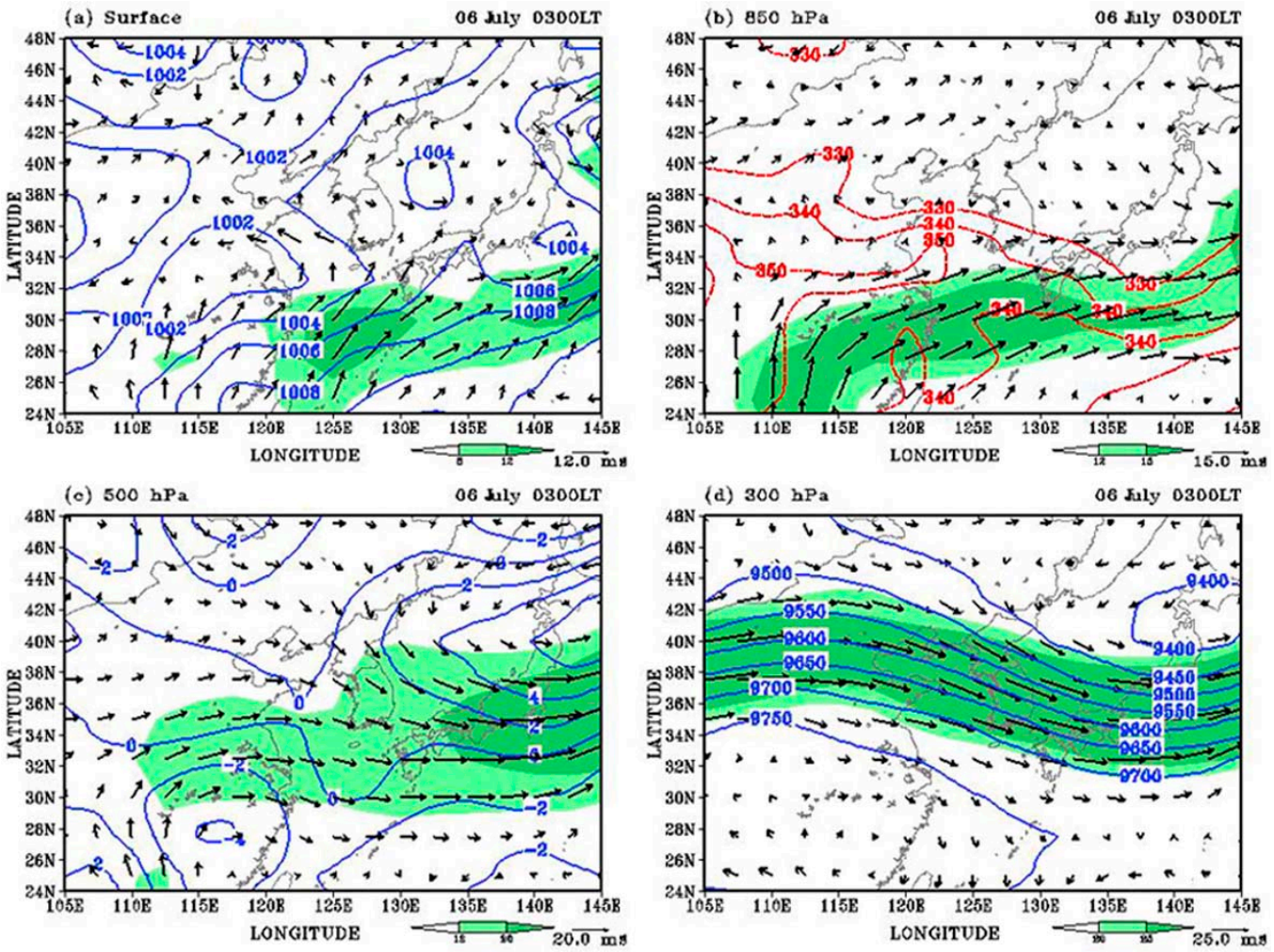

Fig. 5. (a) Pressure (hPa) and wind vector at surface, (b) equivalent potential temperature (K) and wind vector at 850 hPa, (c) relative vorticity and wind vector at 500 hPa, and (d) geopotential height (gpm) and wind vector at 300 hPa at 0300 LST July 6, 2007.

(a) 2100 LST, July 5 (b) 0300 LST, July 6 (c) 0900 LST, July 6

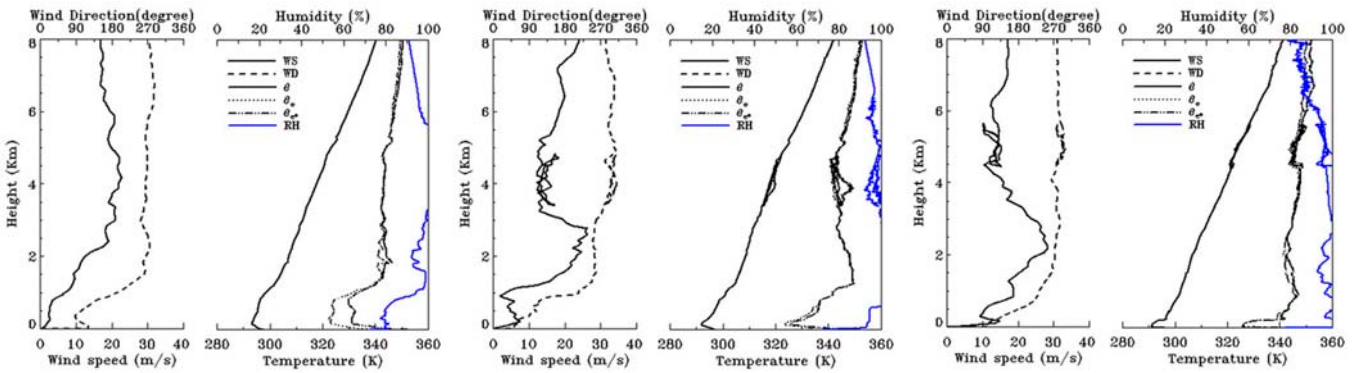

Fig. 6. The vertical profiles of wind speed, wind direction, potential temperature θ, equivalent potential temperature θ_e, saturated equivalent potential temperature θ_e^*, and relative humidity from radio sonde.

cells were located at the south-western of Chujado and moved to north-eastward and south-eastward (Fig. 4). At 2300 LST July 5 (case 1), rainfall system was located at Chujado and Jeju island. At 0100 LST July 6 (case 2), there is no rainfall system over Chujado area but convective cells are located at the western part of Chujado. After 1100 LST July 6 (case 3), there is no significant

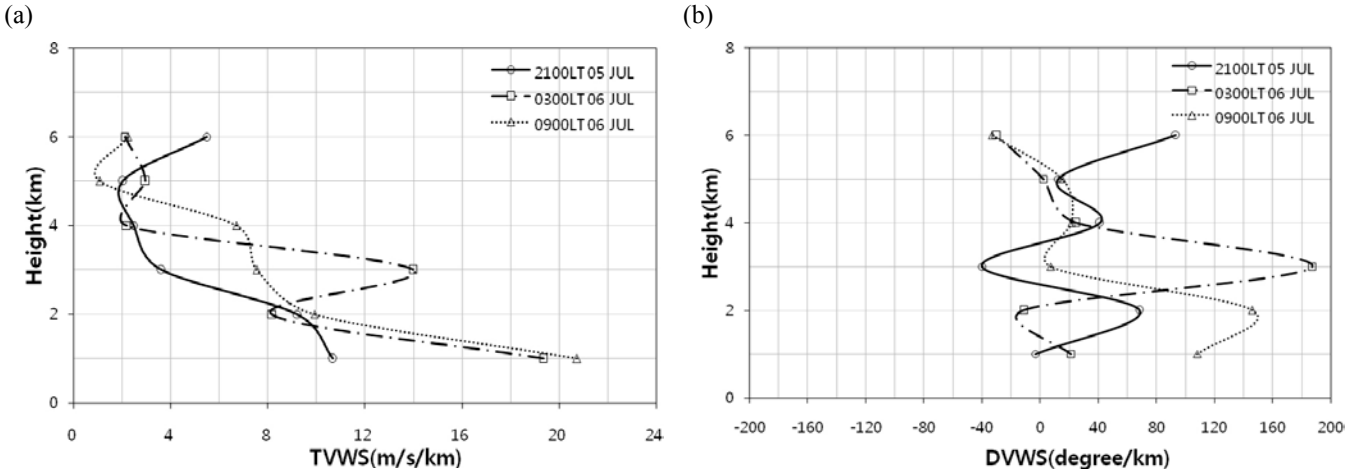

Fig. 7. (a) The total vertical wind shear (TVWS) and (b) directional vertical wind shear (DVWS) obtained from radio sonde.

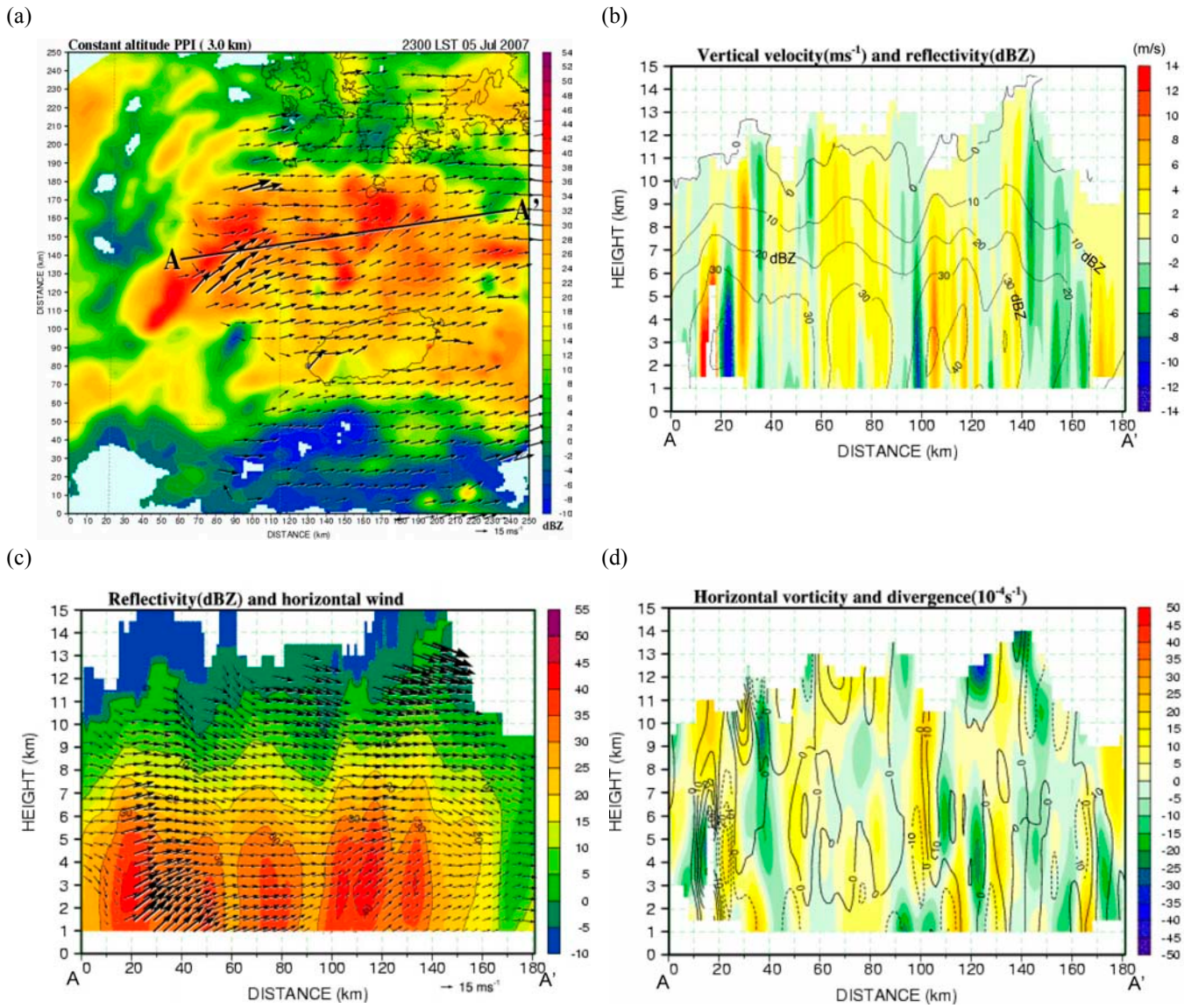

Fig. 8. (a) The reflectivity and horizontal wind field at the 3 km CAPPI at 2300 LST July 5, 2007. Vertical cross sections along A-A'. (b) vertical velocity and reflectivity (contour), (c) horizontal wind and reflectivity, and (d) horizontal vorticity and divergence (contour).

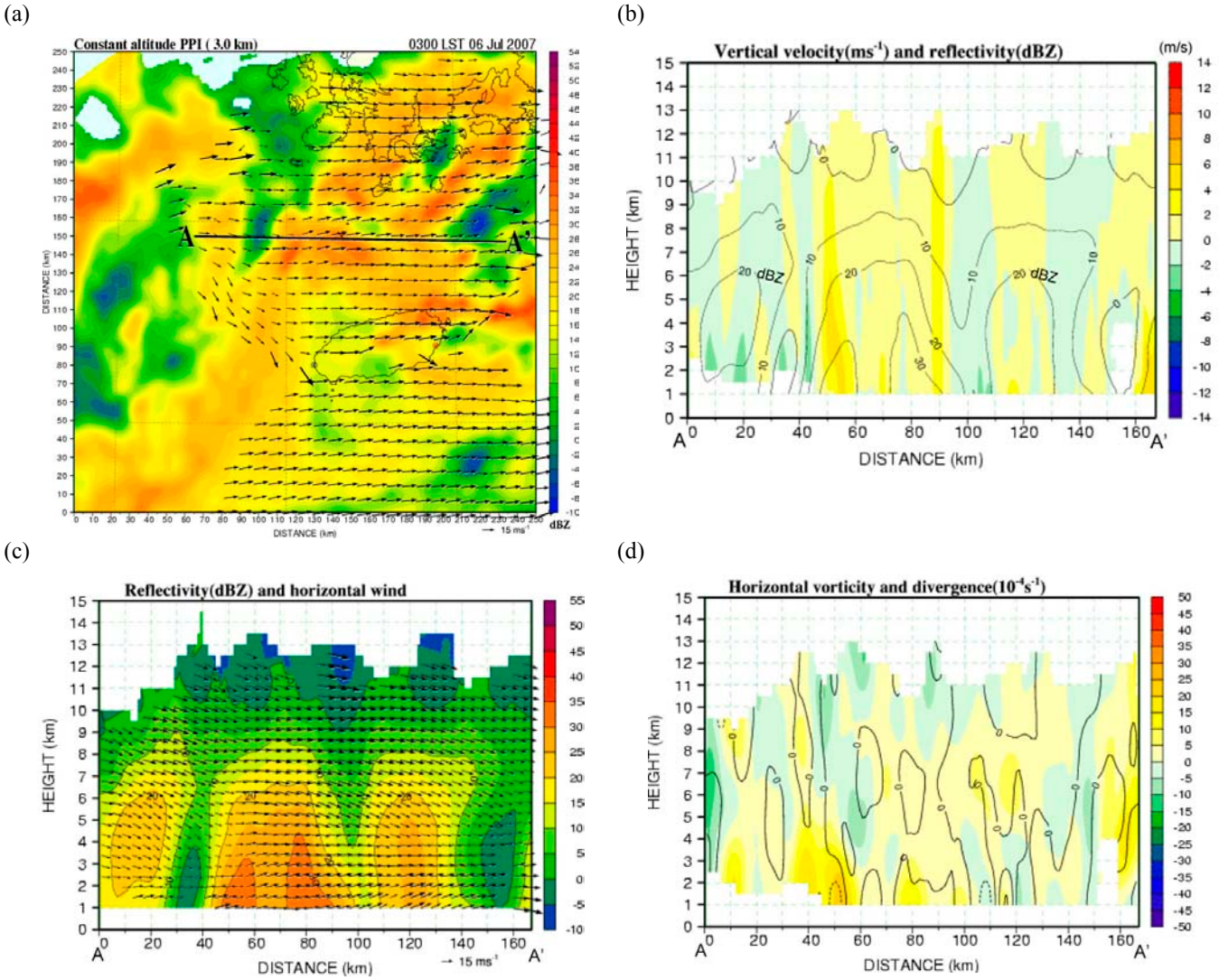

Fig. 9. Same as Fig. 8 but for 0300 LST July 6, 2007.

convective system around Chujado.

The surface weather map shows that southerly wind appears in Chujado area due to the low pressure located at the western part of Jejudo (Fig. 5a). There is convergence over Korean peninsular. At 850 hPa level, a strong wind higher than 15 m s^{-1} appears over the whole southern part of Korea (Fig. 5b). The equivalent potential temperature gradient is about 12 K in the south-western part of Jejudo. The analysis area is covered with weak positive relative vorticity and the westerly wind is over 15 m s^{-1} (Fig. 5c). Strong vertical wind shear would occur since westerly wind in upper atmosphere and south-westerly at surface level. Upper level jet passed through Korean peninsula and geopotential height at Chujado is between 9659 and 9700 (gpm) (Fig. 5d).

The air mass in the troposphere is very humid and there is strong vertical wind shear in the boundary layer below 2 km through out the period. The wind speed became stronger with height reaching 20 m s^{-1} at 4 km. The Lifted Condensation Level (LCL) was 935hPa and the K-Index value was 36 (Fig. 6a). At 0300 LST 6 July, the wind veered from north- easterly to westerly or north-westerly below 4 km and the wind speed was constant below 1 km and became stronger from 1 km to 3 km with height. The LCL was 927 hPa and the value of K-Index was 40 (Fig. 6b). In case 3, the wind speed at the surface was around 10 m s^{-1} and increased with height below 2 km. All the layers below 10 km in height were humid with relative humidity larger than 80% and the radio sonde moved up and down in the height of 4 ~ 6 km because of the strong downdraft. The LCL was 951 hPa and the value of K-Index was 36 (Fig. 6c).

Figure 7 shows the TVWS and DVWS obtained from radio sondes for cases 1, 2, and 3 (at 2100 LST 5 July, 0300 LST, and 0900 LST 6 July). The TVWS is highest at the lower level and decrease with height through the period. The high TVWS at case 2 (0300 LST 6 July) is due to the presence of the lower level jet.

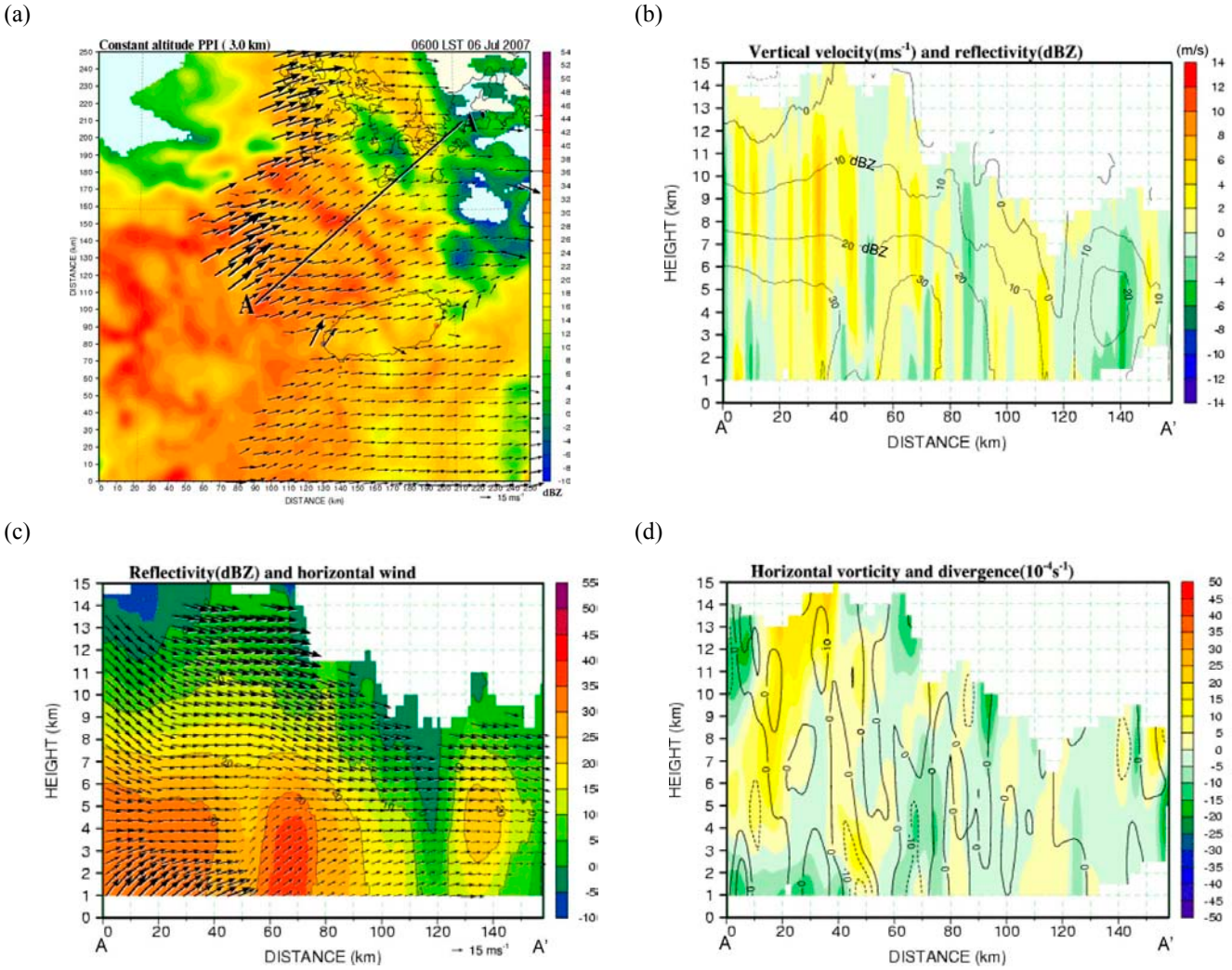

Fig. 10. Same as Fig. 8 but for 0600 LST July 6, 2007.

In case 1 (at 2100LST 05 July), the DVWSs were -3.3, 68.2, -40.1, and 41.2° km^{-1} at 1, 2, 3, and 4 km, respectively. It means that the cold (warm) advection appeared at 1 km and 3 km (2 km and higher than 4 km). In case 2 (at 0300 LST 6 July), the DVWS was 20.9° km^{-1} at 1 km, -11.2° km^{-1} at 2 km, and 186.9° km^{-1} at 3 km. It means that the warm advection dominated at all layers except for 2 km. In case 3 (at 6 July, 0900 LST), the DVWS was 108.2° km^{-1} at the height of 1 km and the positive DVWS dom inated in the whole layer, which means the warm advection was significant at all layers except for 6 km.

Dual Doppler analysis using Gosan and Seongsan S-band Doppler weather radars were carried out to understand the general kinematic characteristics of each rainfall system. In case 1 (at 2300 LST), horizontal convergence occurred in the western part of Chujado. The rainfall system moves into the north-eastern part (Fig. 8a). In the range of 10 to 30 km of the cross section A-A' in Fig. 8a, both strong updraft and downdraft greater than ±10 m s^{-1} appear next to each other (Fig. 8b). The echo top height of 30 dBZ reached to nearly 6 km and the strong south-westerly wind is about 30 m s^{-1} (Fig. 8c). The convergence is from 10 to 30 ($\times 10^{-4}$ s^{-1}) and horizontal vorticity is 20 ($\times 10^{-4}$ s^{-1}) within 20 km from "A" point (Fig. 8d). The updraft, convergence, and horizontal vorticity near Chujado were around 5 m s^{-1}, 10 ($\times 10^{-4}$ s^{-1}), and 5 to 15 ($\times 10^{-4}$ s^{-1}), respectively.

In case 2, the precipitation system with relatively weaker intensity and wind speed than at case 1 moved into the east (Fig. 9a). The downdraft less than 4 m s^{-1} was dominated within 20 km from A as shown in Fig. 9b. The echo top of 30 dBZ was located around 4 km and the wind direction with height was almost constant (Fig. 9c). The convergence was not significant and horizontal vorticity was 15 ($\times 10^{-4}$ s^{-1}) within the range of 20 km from "A" (Fig. 9d). The updraft and horizontal vorticity near Chujado were around 3 m s^{-1} and -1 to 15 ($\times 10^{-4}$ s^{-1}), respectively.

In case 3, rainfall system moves to the east or north-eastward and strong wind speed reaches greater than 15 m s^{-1} (Fig. 10a). The downdraft and updraft with 4 to 6 m s^{-1} occurrs in the range

(a)

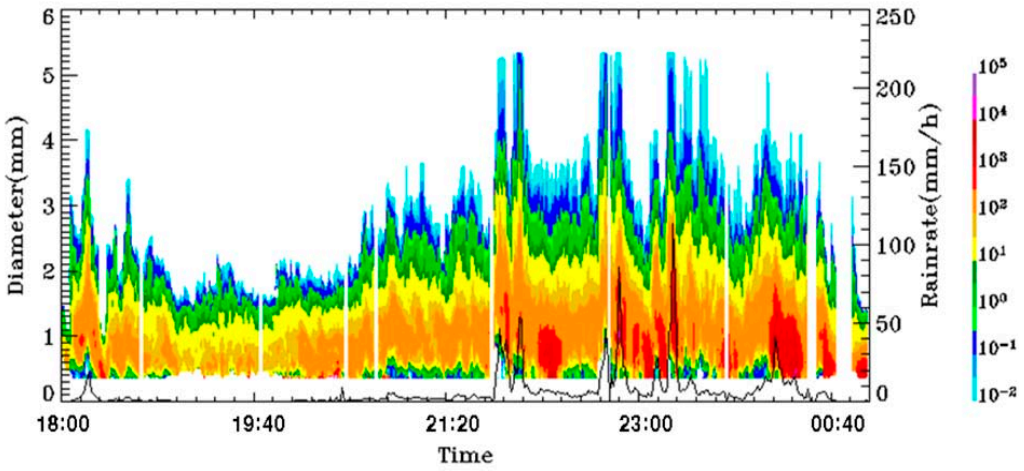

(b)

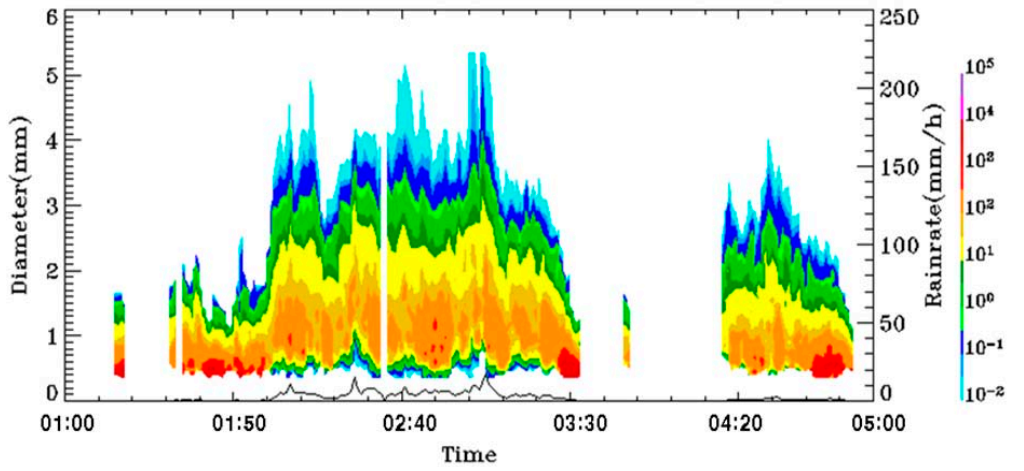

(c)

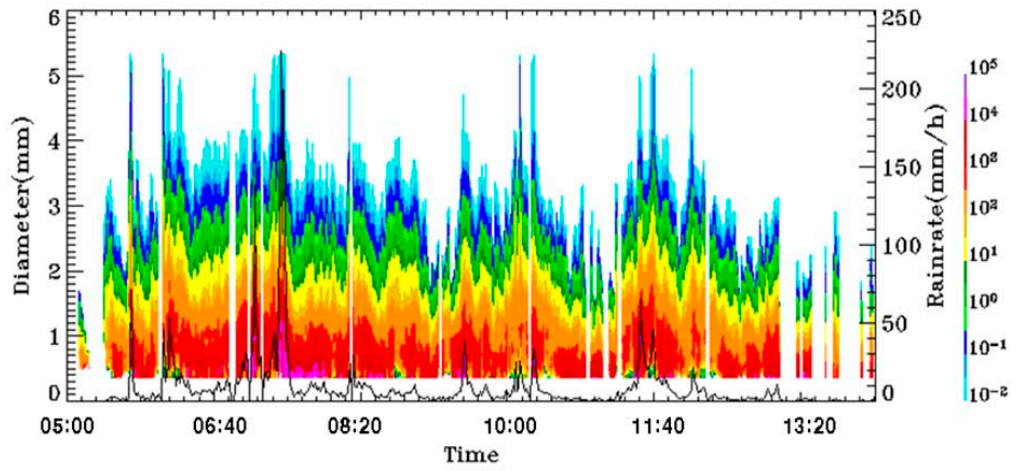

Fig. 11. The time series of rain drop size (left axis) and rainrate (right axis) derived from POSS (a) case 1, (b) case 2, and (c) case 3. The color scale represents number concentration of rain drop and solid line shows rainrate.

between 40 and 60 km from "A" and 30 dBZ echo top exists around 6 km in height (Fig. 10b). In Fig. 10c, south-westerly winds prevails at the surface and at higher height north-west winds more than 15ms^{-1} were seen, at the range of 40km from "A". The convergence of 10 ($\times 10^{-4}$ s^{-1}) occurs near 3km in the range between 40 and 60 km from "A" (Fig. 10d). The updraft,

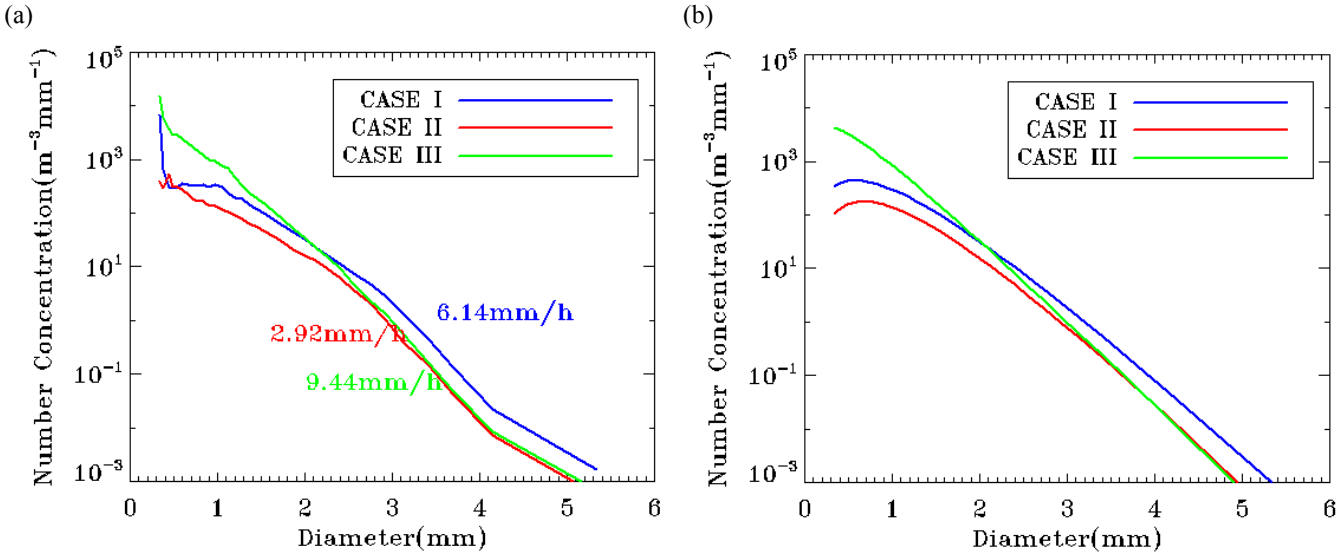

Fig. 12. Averaged DSD from (a) POSS disdrometer and (b) gamma distribution.

convergence, and horizontal vorticity near Chujado were around 3 m s^{-1}, 10 ($\times 10^{-4}$ s^{-1}), and -10 to 5 ($\times 10^{-4}$ s^{-1}), respectively.

Figure 11 shows the time series of rainrate and number concentration of raindrop with size obtained from POSS. The maximum rainrates for one minute of each case are 113.6, 18.1 and 224.3 mm h^{-1}, respectively. The rain drop numbers of rain drop less than or equal to 2 mm and larger than 2 mm are very different with cases. Figure 12 shows that the averaged DSDs obtained from a POSS disdrometer and gamma model for 402, 171, and 485 minutes, respectively. The mean rainrate of each case was 6.14, 2.92, and 9.44 mm h^{-1}. In all cases, the shape of DSDs has the exponential fitting except for smaller drop sizes.

However, there is significant difference of number concentrations before and after 2 mm drop in diameter between case 1 and case 3. The drops smaller than 2 mm in diameter were contributed to case 3 and larger ones than 2 mm were contributed to case 1. This tendency is also shown in Fig. 12b. It is considered in a simple sense that rain drops in case 1 would be affected by coalescence which decreases the numbers of small size drops and increase those of the larger drops. The DSDs in case 3 would be affected by break-up which increases the numbers of small size drops and decreases the numbers of large size drops. The shapes of each case are 2.14, 2.79, and 0.8, respectively. The slopes are 3.72, 4.13, and 3.81 and the intercepts are 12469, 8679, and 38248, respectively. Parameters of each gamma fitting are summarized in Table 1.

Table 1. The characteristics of each case obtained from DSDs.

	CASE 1	CASE 2	CASE 3
Shape	2.14	2.79	0.8
Slope	3.72	4.13	3.81
Intercept	12469	8679	38248
Sample No.	402	171	485

4. Concluding remarks

To understand characteristics of precipitation system accompanied with Changma front, three rainfall cases of a single precipitation system associated with the Changma front were identified and analyzed by using rain gauge data, radio sonde data, POSS, weather radar and NCEP/NCAR reanalysis data. The schematic view of precipitation system accompanied by Changma front from 5 to 6 July in 2007 is shown in Fig. 13. The cold (warm) advection appeared at 1 km and 3 km (2 km and higher than 4 km), the updraft was distributed 10 to 14 m s^{-1}, and the 30 dBZ echo top height reached to nearly 6 km in case 1. In case 2, the warm advection dominated at all layers except for 2 km, the updraft was 2 to 4 m s^{-1}, and the echo top of 30 dBZ was around 4 km. In case 3, the warm advection was significant at all layers, the updraft was around 4 to 6 m s^{-1}, and 30 dBZ echo top existed around 6 km in case 3. The mean rainrate of each case was 6.14, 2.92, and 9.44 mm h^{-1}, respectively.

In this study, the deep warm advection is shown to be associated with a rainfall system of longer duration and stronger rainrate but smaller size diameter of raindrop as shown in case 3. The instability, which means the cold advection at the surface and the warm advection at higher layer, would make larger size diameter of raindrop contributed to the rainfall system as occurred in case 1. The echo top height of 30 dBZ was around 6 km in the two well developed rainfall systems and around 4 km in the rainfall system which had not significant rainfall amount. The number concentrations of raindrop has turning point at the drop size of 2 mm in diameter. The stronger (weaker) updraft and downdraft

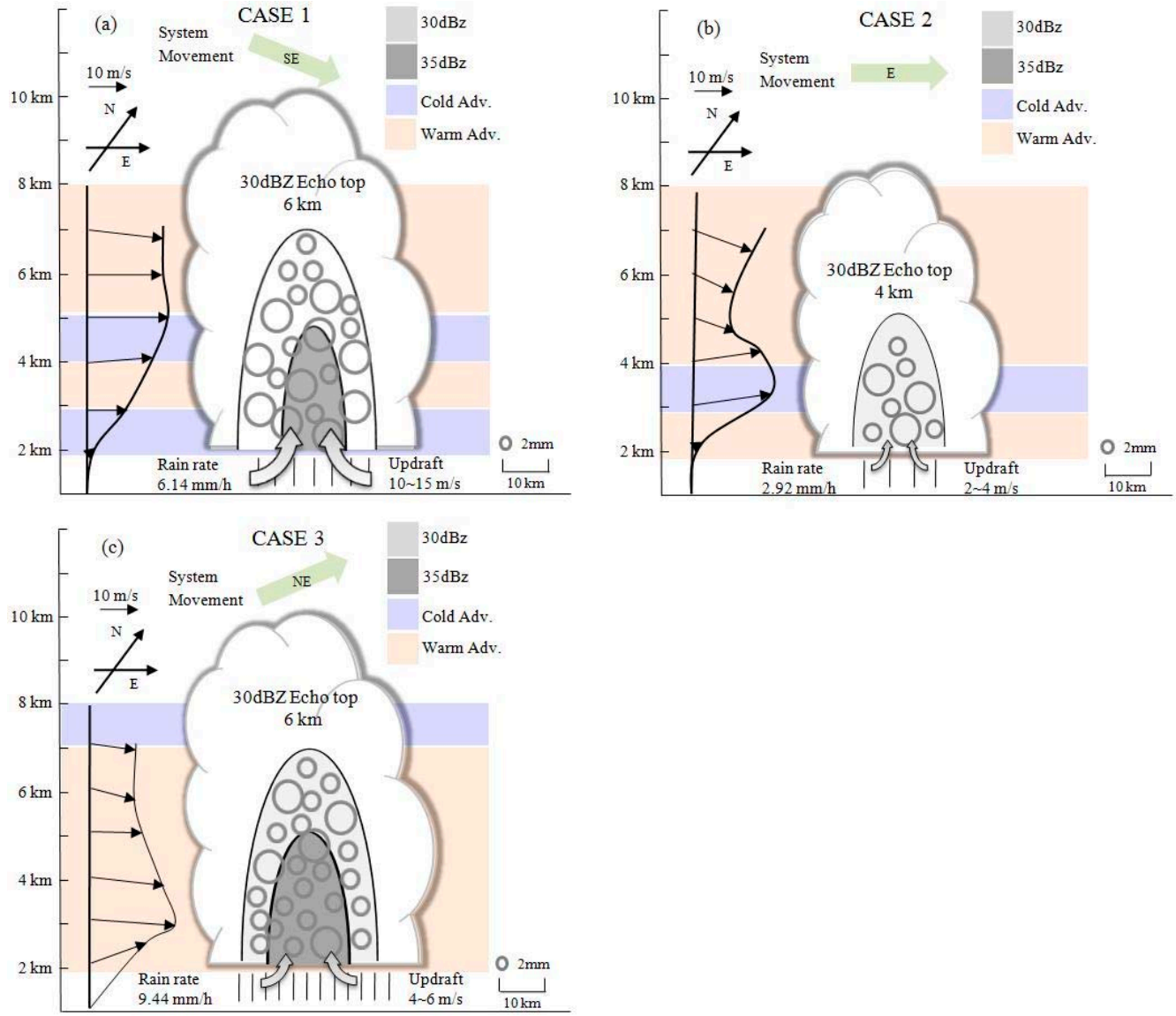

Fig. 13. Schematic diagram of three identified rainfall systems of the observed Changma front, (a) case 1, (b) case 2, and (c) case 3, respectively

were also related to the decreased number concentration of smaller (larger) size drops and increased that of the larger (smaller) drops. The characteristics of mesoscale precipitation system may need further study at smaller scales by analyzing the system for shorter time and focusing on the precipitation appearance like band shape type with its orientation as it is propagating, because this study was limited to three cases.

Acknowledgements. This research was supported by the National Research Foundation of Korea (NRF) through a grant provided by the Korean Ministry of Education, Science & Technology (MEST) in 2009 (No. K2 0607010000). We thank to the Korean Meteorological Administration for providing data and the National Center for Environmental Protection for the reanalysis data.

REFERENCES

Akiyama, T., 1973: The large-scale aspects of the characteristics features of the Baiu front. *Pap. Meteorol. Geophys.*, **24**, 157-188.

Armijo, L., 1969: A theory for the determination of wind and precipitation velocities with Doppler radars. *J. Atmos. Sci.*, **26**, 570-575.

Biggerstaff, M. I., and R. A., Houze Jr., 1991: Kinematic and precipitation structure of the 10-11 June, 1985 squall line. *Mon. Wea. Rev.*, **119**, 3034-3065.

Choi, Y. J., and J. C., Nam, 2006: Introduction of phase I KEOP. *Proc. Spring Meeting of Korean Meteor. Soc.*, Gwangju, Korea, KMS, 384-385. (in Korean)

Ding, Y. H., and J. C. L. Chan, 2005: The East Asian summer monsoon:

an overview, *Meteor. Atmos. Phys.*, **89**, 117-142.

_____, C. Y. Li, and Y. J. Liu, 2004: Overview of the South China Sea monsoon experiment. *Adv. Atmos. Sci.*, **21**, 343-360.

Holton, J. R., 1979: *An Introduction to Dynamic Meteorology*. Academic Press, 391 pp.

Ishihara, M., A. Tabata, K. Akaeda, T. Yokoyama, and H. Sakakibara, 1992: The structure of a subtropical squall line observed with a Doppler radar. *Tenki*, **39**, 727-743. (in Japanese)

_____, Y. Fujiyoshi, A. Tabata, H. Sakakibara, K. Akaeda, and H. Okamura, 1995: Dual Doppler radar analysis of an intense mesoscale rainband generated along the Baiu front in 1988: Its kinematical structure and maintenance process. *J. Meteor. Soc. Japan*, **73**, 139-163.

Kim, S. S., C. H. Chung, S. U. Park, and B. S. Lee, 1983: The characteristic structural differences of the rainy front (Changma front) between the wet and dry seasons. *J. Korean Meteor. Soc.*, **19**, 12-32. (in Korean with English abstract)

Kozu, T., and K. Nakamura, 1991: Rainfall parameter estimation from dual-radar measurements combining reflectivity profile and path-integrated attenuation. *J. Atmos. Oceanic Technol.*, **8**, 259-271.

Lau, K. M., Y. H. Ding, J. T. Wang, R. Johnson, R. Cifelli, J. Gerlach, O. Thjiely, T. Rikebbach, S. C. Tsay, and P. H. Lin, 2000: A report of the field operation and early results of the South China Sea monsoon experiment (SCSMEX). *Bull. Amer. Meteor. Soc.*, **81**, 1261-1270.

Lee, D. K., H. R. Kim, and S. Y. Hong, 1998: Heavy rainfall over Korea during 1980-1990. *Korean J. Atmos. Sci.*, **1**, 32-50.

Lin, Y. J., R. W. Pasken, and H. W. Chang, 1991: The structure of a subtropical prefrontal convective rainband. Part I: Mesoscale kinematic structure determined from dual Doppler measurements. *Mon. Wea. Rev.*, **120**, 1816-1836.

Matsumoto, S., S. Yoshizumi, and M. Takeuchi, 1970: On the structure of the "Baiu Front" and the associated intermediate scale disturbances in the lower atmosphere. *J. Meteor. Soc. Japan*, **48**, 479- 491.

_____, _____, and _____, 1971: Characteristic feature of Baiu front associated with heavy rainfall. *J. Meteor. Soc. Japan*, **49**, 267-281.

Miller, L. J., and S. M. Fredric, 1998: Custom Editing and Display of Reduced Information in Cartesian space (CEDRIC) manual. National Center for Atmospheric Research, 130 pp.

Moteki, Q., H. Uyeda, T. Maesaka, T. Shinoda, M. Yoshizaki, and T. Kato, 2004: Structure and development of two merged rainbands observed over the East China Sea during X-BAIU-99 PART I: Meso-β-scale structure and development processes. *J. Meteor. Soc. Japan*, **82**, 19-24.

NCAR, 1999: Sorted Position Radar Interpolation (SPRINT) manual. National Center for Atmospheric Research, 76 pp.

Ninomiya, K., 1978: Heavy rainfalls associated with frontal depression in Asia subtropical humid region. PART I: Synoptic-scale features. *J. Meteor. Soc. Japan*, **56**, 253-266.

_____, and T. Akiyama, 1992: Multi-scale features of Baiu, the Summer Monsoon over Japan and East Asia. *J. Meteor. Soc. Japan*, **70**, 467-495.

O'Brien, J. J., 1970: Alternative solution to the classical vertical velocity problem. *J. Appl. Meteorol.*, **9**, 197-203.

Oh, J. H., W. T. Kwon, and S. B. Ryoo, 1997: Review of the researches on Changma and future observational study (KORMEX). *Adv. Atmos. Sci.*, **14**, 207-222.

Ray, P. S., K. K. Wagner, K. W. Johnson, J. J. Stephens, W. C. Bumgarner, and E. A. Mueller, 1978: Triple-Doppler observations of a convective storm. *J. Appl. Meteorol.*, **17**, 1201-1212.

_____, C. L. Ziegler, W. Bumgarner, and R. J. Serafin, 1980: Single- and multiple-Doppler radar observations of tornadic storms. *Mon. Wea. Rev.*, **108**, 1607-1625.

_____, A. Robinson, and Y. Lin, 1991: Radar analysis of a TAMEX frontal system. *Mon. Wea. Rev.*, **119**, 2519-2539.

Takahashi, N., H. Uyeda, K. Kikuchi, and K. Iwanami, 1996: Mesoscale and convective scale features of heavy rainfall events in lat period of the Baiu season in July 1988, Nagasaki Prefecture. *J. Meteor. Soc. Japan*, **74**, 539-561.

Teng, J. H., C. S. Chen, T. C. C. Wang, and Y. L. Chen, 2000: Orographic effects on a squall line system over Taiwan. *Mon. Wea. Rev.*, **128**, 1123-1138.

Ulbrich, C. W., 1983: Natural variations in the analytical form of the raindrop size distribution. *J. Climate Appl. Meteor.*, **22**, 1764-1775.

Yoshizaki, M., T. Kato, Y. Tanaka, H. Takayama, Y. Shoji, H. Seko, K. Arao, K. Manabe, and Members of X-BAIU-98 Observation, 2000: Analytical and numerical study of the 26 June 1998 orographic rainband observed in Western Kyushu, Japan. *J. Meteor. Soc. Japan*, **78**, 835-856.